PHYSICAL REVIEW B VOLUME 44, NUMBER 15 15 OCTOBER 1991-I

# Structure, growth, and bonding nature of Mg clusters

Vijay Kumar* and Roberto Car†
*International School for Advanced Studies, 34014 Trieste, Italy*
*and International Centre for Theoretical Physics, 34100 Trieste, Italy*
(Received 6 March 1991)

The structure, growth, and bonding nature of $Mg_n$ ($n$ = 2–13) clusters is studied using the density-functional molecular-dynamics method and the simulated annealing technique within the local-density approximation. We find a tetrahedron and a trigonal prism as two important constituents of the structure of Mg clusters to which atoms can be added by capping the faces. $Mg_{13}$ is neither an icosahedron nor a cuboctahedron. The lowest-energy structure of $Mg_{13}$ that we obtained from our simulated annealing can be considered as fusion of $Mg_9$ and $Mg_4$ clusters. This is nearly degenerate with the relaxed hcp structure and suggests the possibility of a path for transition to hcp structure for bigger clusters. We find $Mg_4$ and $Mg_{10}$ to be the magic clusters, which is in general agreement with the predictions of the jellium model of metal clusters. However, calculations of the charge densities, the $p$ character, and the gap between the highest occupied and the lowest unoccupied states suggest the presence of mixed bonding character in Mg clusters and an oscillatory and slow convergence to bulk metallic behavior.

## I. INTRODUCTION

In recent years intense research has been going on[1–5] to study clusters of different materials in order to understand their physical properties and evolution to bulk behavior. This has also led to the possibility of making some novel materials.[6] An interesting aspect of these studies is the different nature of chemical bonding for small clusters of some elements. For example, small Si clusters have close-packed metalliclike structures,[7–9] whereas neutral dimers of divalent metals such as mercury and magnesium are very weakly bonded, due to $ns^2$ closed-shell atomic electronic structure and large promotional energy, to the $p$ state. Therefore for such elements a transition to bulk chemical bonding should occur as the cluster size grows. Studies on Si clusters indicate that transition to diamondlike open structure should occur for large clusters. The estimate of the cluster size for this transition varies from a few tens[9] to several hundred[8] atoms. Recent calculations[10] on clusters with up to 45 atoms show no sign of diamond structure. On the other hand, experimental studies on mercury clusters[11] suggest transition from van der Waals to metallic behavior for a moderate size of the clusters ($70 \geq n \geq 13$), which makes their theoretical study attractive. Also the magic numbers for the van der Waals bonded clusters and clusters of the free-electron-like metals such as Na are very different. Therefore the information available on the stability of the van der Waals bonded clusters as well as clusters of the free-electron-like metals[12] can be quite helpful for understanding this transition.

So far very little is known about the nature of transition from van der Waals to metallic behavior in clusters of group-2 elements. Dimers of group-2A elements have been studied by several groups. It has been the general view[13] that bonding in dimers of group-2A elements is due to van der Waals forces according to which the bond strength should increase in the order $Be_2 \rightarrow Mg_2 \rightarrow Ca_2 \rightarrow \cdots$, due to the corresponding increase in the atomic polarizabilities.[14] However, studies[15] within the local-spin-density (LSD) approximation predict a stronger bond for $Be_2$ than for $Mg_2$. The binding energy trends of dimers obtained from the LSD calculations are similar to those observed in the bulk cohesive energy[16] and also agree with available experimental results.[17,18] Thus while the binding energy is overestimated in the local-density approximation (LDA), one can hope to achieve the trends satisfactorily. For clusters detailed studies have been done for the equilibrium structures of $Mg_n$ (Ref. 19) and $Be_n$ (Ref. 20) ($n \leq 7$) but these do not provide much information regarding their magic numbers, growth, and transition to metallic bonding. These studies, however, do suggest[21] that the transition to bulklike bonding in Mg clusters is slower than in the case of Be. Very recently Kawai and Weare[22] (KW) have studied berillium clusters with up to 20 atoms. They find bulklike structural features for clusters having around 11 atoms and the $p$ character of the electronic charge density is found to be close to its bulk value even for a 6-atom cluster. For $Mg_n$ clusters there is no published systematic study with $n > 7$. It would be of interest to understand the growth and transition to metallic behavior in clusters of different divalent metals as their bulk structure varies from hcp to fcc to bcc for

 

group-2A elements and hcp to rhombohedral for group-2B elements. Here we present results of such a detailed study for magnesium clusters with up to 13 atoms. While no experimental results on the abundance of magnesium clusters are available, our studies were also motivated from the need to understand the stability of icosahedral order in Al-Mg based quasicrystals,[23] as in these alloys clusters with icosahedral symmetry are abundant in crystalline, amorphous, and quasicrystalline phases.[24] This suggests that icosahedral clusters of Al-Mg and related alloys may be particularly stable. Therefore a knowledge of the structures and energetics of clusters of individual components will be helpful in understanding the role of the electronic structure and atomic size in icosahedral packing.

We have used the density-functional molecular-dynamics technique[25] to explore the equilibrium structures within the framework of the simulated annealing and the LDA. This method has been successfully applied in recent years to study equilibrium geometries of Si,[7,10,26] Se,[27] S,[28] Na,[29] P,[30] Be,[22] and mixed clusters of GaAs (Ref. 31) and NaK.[29] Results of such calculations agreed with experiments wherever available. Our results for the lowest-energy structures of Mg clusters suggest a growth by the capping of a tetrahedron (for $n \leq 8$) or a trigonal prism (for $n > 8$). $Mg_{13}$ is found to be neither an icosahedron nor a cuboctahedron. It can be described as a result of the fusion of a tricapped trigonal prism and a tetrahedron. Calculations of the cohesive energy, the gap between the highest occupied, and the lowest unoccupied Kohn-Sham eigenvalues and the $p$ character of the electronic charge density suggest that the transition to the bulk behavior is slow and oscillatory. We also present results of the chemisorption energy as a function of the cluster size. We hope these will be of general interest in understanding the chemisorption behavior of clusters. A preliminary report of these results was presented elsewhere[32] whereas a summary of our main results has been presented in Ref. 33.

This paper is organized as follows. In Sec. II we present some technical details of our calculational procedure. In Sec. III results of the structure, growth, relative stability, bonding nature, chemisorption energies, and fragmentation channels are presented. Section IV contains a discussion and our conclusions.

## II. CALCULATIONAL PROCEDURE

The *ab initio* molecular-dynamics (MD) method[25] provides an efficient way for optimization of energy with respect to electronic and ionic degrees of freedoms simultaneously within the density-functional formulation. While the details can be found elsewhere[25,28,34] we present here the basic equations for the sake of completeness. In this method the electronic degrees of freedom $\psi_i$ and the ionic degrees of freedom $\mathbf{R}_I$ in the energy functional $E[\{\psi_i\},\{\mathbf{R}_I\}]$ are taken to be time dependent and a Lagrangian is introduced:

$$L = \sum_i^{\text{occ}} \int d\mathbf{r}\, \mu_i |\dot{\psi}_i(\mathbf{r})|^2 + \tfrac{1}{2}\sum_I M_I \dot{\mathbf{R}}_I^2 - E[\{\psi_i\},\mathbf{R}_I] + \sum_{i,j} \Lambda_{ij}\left(\int d\mathbf{r}\psi_i^*(\mathbf{r})\psi_j(\mathbf{r}) - \delta_{ij}\right) \quad (1)$$

which generates a dynamics for the parameters $\psi_i$ and $\mathbf{R}_I$ through the equations of motion:

$$\mu_i \ddot{\psi}_i(\mathbf{r},t) = -\frac{\delta E}{\delta \psi_i^*(\mathbf{r},t)} + \sum_j \Lambda_{ij}\psi_j(\mathbf{r},t) \quad (2a)$$

and

$$M_I \ddot{\mathbf{R}}_I = -\frac{\delta E}{\delta \mathbf{R}_I(t)}, \quad (2b)$$

where $M_I$ are the ionic masses and $\mu_i$ are the fictitious masses for the electronic degrees of freedom which we have taken to be independent of the state $i$. $\Lambda_{ij}$ are the Lagrangian multipliers for the orthonormalization of the single-particle orbitals $\psi_i$. The energy functional $E$ is given by

$$E[\{\psi_i\},\{\mathbf{R}_I\}] = \sum_i^{\text{occ}} f(i)\int d\mathbf{r}\,\psi_i^*(\mathbf{r})(-\tfrac{1}{2}\nabla^2)\psi_i(\mathbf{r}) + \int d\mathbf{r}\, V^{\text{ext}}(\mathbf{r})n(\mathbf{r}) + \tfrac{1}{2}\int d\mathbf{r}\,d\mathbf{r}'\frac{n(\mathbf{r})n(\mathbf{r}')}{|\mathbf{r}-\mathbf{r}'|} + E^{\text{xc}}[n(\mathbf{r})] + \tfrac{1}{2}\sum_{I\neq J}\frac{Z_I Z_J}{|\mathbf{R}_I - \mathbf{R}_J|}, \quad (3)$$

where atomic units $e = \hbar = m_e = 1$ are used. $E^{\text{xc}}[n]$ is the exchange-correlation energy which has been calculated within the LDA. Perdew and Zunger[35] parametrization of the Ceperley and Alder[36] data was used for the exchange correlation. $V^{\text{ext}}(\mathbf{r})$ is the total external potential felt by the electrons and $n(\mathbf{r})$ is the charge density defined as

$$n(\mathbf{r}) = \sum^{\text{occ}} f(i)|\psi_i(\mathbf{r})|^2, \quad (4)$$

where $f(i)$ is the occupation number for the state $i$. We have used the *ab initio* norm-conserving pseudopotentials of Bachelet, Hamann, and Schlüter[37] for the electron-ion interaction and therefore $Z_I$ represents the ionic pseudocharge. In order to speed up the calculations we adopted the Kleinman and Bylander[38] separable representation for the pseudopotential and considered only $s$ nonlocality. Test calculations on $Mg_2$ showed that the effect of the inclusion of $p$ nonlocality was negligible. The

cluster was placed in a fcc unit cell with a lattice constant of 46 a.u. The size of the cell was large enough so that the interaction between a cluster and its periodic images was negligible. A plane-wave expansion with an energy cutoff of 8 Ry was used[39] with the Γ point to sample the Brillouin zone of the molecular-dynamics supercell. All calculations have been performed for the singlet state. Spin-polarization effects were studied by Reuse *et al.*[19] for smaller clusters and the lowest-energy state was found to be a singlet.

During the molecular-dynamics runs the integration time for the electronic degrees of freedom was taken to be $6 \times 10^{-16}$ sec and the fictitious mass $\mu$ was taken to be 3750 a.u. Calculations on smaller clusters ($n \leq 5$) were done using the steepest-descent approach for a few selected geometries. For $n > 5$, however, the simulated annealing technique was used to explore the complicated energy surface. In this technique the cluster was heated up to 1000 K (for n=6) and 1500 K (for $n > 6$) for about 1000 time steps which was sufficient to make ions diffuse. The system was then allowed to evolve for 2500–3000 time steps. During this period the system lost completely the memory of its starting configuration. Subsequently it was cooled with a quenching rate of $1.66 \times 10^{14}$ K/sec. For all clusters with $n \leq 10$, the system remained on the Born-Oppenheimer surface and only occasional electron minimizations were done during all the MD runs. For $n > 10$, however, electron minimizations were required more often to ensure adiabatic evolution. As we shall discuss, this is related to the changes in the electronic structure of the clusters.

## III. RESULTS

### A. Structure and growth of $Mg_2$-$Mg_{13}$ clusters

In the following we present structures of clusters obtained from the steepest-descent technique for some selected geometries ($n \leq 5$) and the simulated annealing procedure ( $n > 5$). For larger clusters in addition a few geometries were also studied with the steepest-descent technique. In almost all cases[40] the simulated annealing procedure gave the lowest-energy structures. These can be described in terms of a tetrahedron and a trigonal prism. In Table I we have listed all the structures studied and their cohesive energies. In the following we present these results in detail.

#### *1. $Mg_2$-$Mg_5$*

The equilibrium structures of $Mg_2$-$Mg_5$ clusters are shown in Fig. 1. As it is known, $Mg_2$ is very weakly bonded with a bond length of 6.33 a.u. [Fig. 1(a)]. Experimentally $Mg_2$ is found[17] to have a singlet ground state with a bond length of 7.35 a.u. and cohesive energy 0.025 eV/atom. As discussed before, LDA overestimates the binding energy (Table I). However, our results agree with a recent LSD calculation[19] which gives 0.11 eV/atom and 6.37 a.u., respectively, for the energy and the bond length.

The lowest-energy state that we get for $Mg_3$ is an equilateral triangle [Fig. 1(b)]. The $Mg_3$ chain [Fig. 1(c)] is 0.111 eV/atom higher in energy than the equilateral triangle. Thus the clusters favor to maximize coordination number. This trend is continued for bigger clusters as well. The lowest-energy structure for $Mg_4$ is a regular tetrahedron [Fig. 1(d)]. As we shall discuss later this is a particularly stable cluster with a cohesive energy of 0.53 eV/atom and a considerably smaller bond length. Another calculation with planar geometry finally converged to the tetrahedron implying no energy barrier between the planar and the three-dimensional close-packed structures. This result will be useful later in the discussion of $Mg_{13}$ structure.

For $Mg_5$ three geometries were studied. A slightly elongated trigonal bipyramid has the lowest energy (0.54 eV/atom). Capping a tetrahedron face leads to a contraction of the bonds between the base atoms whereas the other bonds get elongated [Fig. 1(e)]. The square pyramid [Fig. 1(f)] and the pentagon [Fig. 1(g)] are, respectively, 0.117 and 0.179 eV/atom higher in energy than the trigonal bipyramid. All these geometries are in good agreement with a recent LSD calculation.[19] Incidentally, the trigonal bipyramid is also a fragment of the hcp structure, though we must say that the bonding is far away from the bulk behavior. Similar ground-state

TABLE I. Cohesive energies of the singlet states of $Mg_n$ clusters.

| $n$ | Structure | Energy (eV/atom) |
|---|---|---|
| 2 | Dimer | 0.115 |
| 3 | Equilateral triangle | 0.284 |
| | Chain | 0.173 |
| 4 | Regular tetrahedron | 0.530 |
| 5 | Trigonal bipyramid | 0.540 |
| | Square pyramid | 0.423 |
| | Pentagon | 0.362 |
| 6 | Capped trigonal bipyramid | 0.566 |
| | Rectangular base octahedron | 0.562 |
| | Octahedron | 0.422 |
| 7 | Pentagonal bipyramid | 0.649 |
| | Bicapped trigonal bipyramid | 0.630 |
| 8 | Capped pentagonal bipyramid | 0.694 |
| | Relaxed bicapped trigonal prism | 0.676 |
| 9 | Tricapped trigonal prism | 0.809 |
| 10 | Tetracapped trigonal prism | 0.886 |
| | Relaxed geometry of Kawai and Weare[a] | 0.881 |
| 11 | Pentacapped trigonal prism | 0.870 |
| 12 | Capped trigonal prism [Fig. 7(a)] | 0.874 |
| | Relaxed geometry of Kawai and Weare[a] | 0.838 |
| 13 | From simulated annealing | 0.902 |
| | Relaxed hcp | 0.898 |
| | Relaxed fcc | 0.871 |
| | Relaxed icosahedron | 0.859 |
| | Bulk[b] | 1.687 |

[a] Reference 22.

[b] Reference 47.

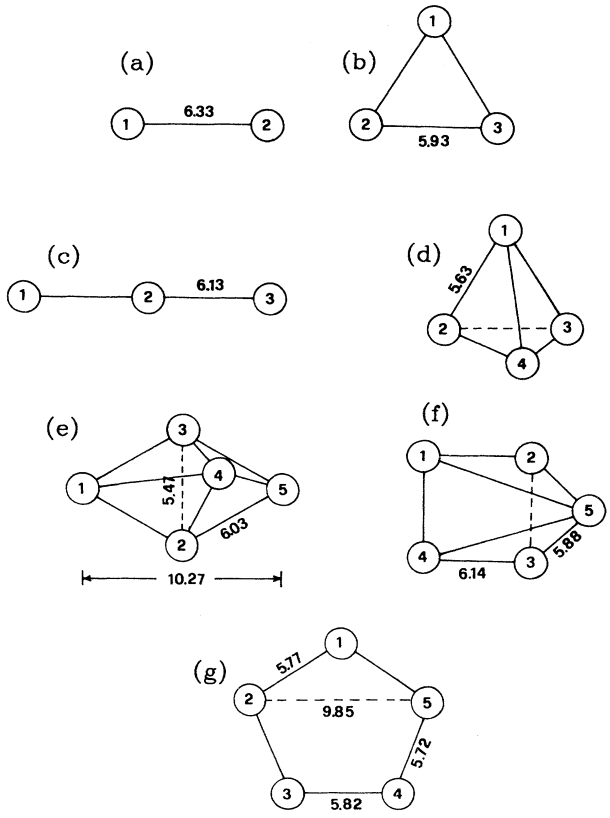


FIG. 1. Structures of $Mg_n$ clusters. (a) $n = 2$; (b) $n = 3$, equilateral triangle; (c) $n = 3$, chain; (d) $n = 4$, regular tetrahedron; (e) $n = 5$, trigonal bipyramid; (f) $n = 5$, square pyramid; (g) $n = 5$, pentagon.

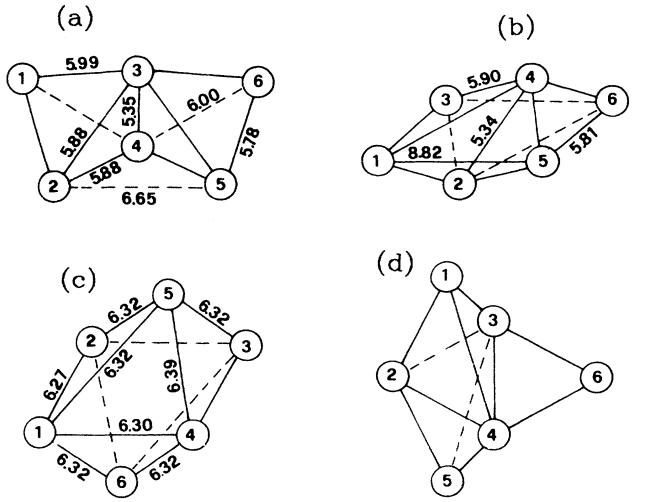


FIG. 2. Structures of $Mg_6$ cluster. (a) From the simulated annealing; (b) rectangular octahedron; (c) a distorted octahedron; (d) a fragment of the hcp structure.

geometries have been obtained for Be clusters[20,22] suggesting similarites of bonding character between the two systems in this size range.

### 2. $Mg_6$

Simulated annealing calculations of the $Mg_6$ cluster yielded a structure shown in Fig. 2(a). This can be obtained by capping a face [3-4-5 in Fig. 1(e)] of the $Mg_5$ trigonal bipyramid. Alternately it can also be viewed as the fusion of two tetrahedra on an edge (3-4) which is substantially shorter than the other bonds. Atoms 3 and 4 have the highest coordination and as we shall discuss later, metallicity develops first in such bonds.

Since the structures for Mg clusters with $n \leq 5$ are very nearly the same as for the van der Waals bonded clusters, it is of interest to study the relative stability of a regular octahedron which has the lowest energy for the van der Waals clusters.[41] Here we present results for two octahedron structures: (1) a rectangular base octahedron and (2) a regular octahedron.

(1) Reuse *et al.*[19] obtained an octahedron with a rectangular base [Fig. 2(b)] to be of lowest energy. We have done a steepest-descent calculation for this structure and find it only very slightly (0.004 eV/atom) higher in energy than the simulated annealing structure. The former can again be considered as two fused tetrahedra since the two sides in the rectangle are quite long leading to only a very weak interaction between the two joining atoms. The number and the lengths of the remaining bonds are nearly the same in the simulated annealing and the rectangular base octahedron structures which can be considered as degenerate.

(2) Steepest-descent calculations for a regular octahedron lead to a slightly distorted octahedron [Fig. 2(c)] which is 0.145 eV/atom higher in energy than the simulated annealing structure. Thus $Mg_6$ is the smallest cluster for which significant difference shows up from the van der Waals bonded clusters. These results also imply that an energy barrier exits between the two octahedral structures. The simulated annealing structure can be obtained from a fragment of the bulk Mg shown in Fig. 2(d). It is evident from Fig. 2(d) that by bringing atoms 5 and 6 closer to each other we obtain the structure of Fig. 2(a).

### 3. $Mg_7$

For $Mg_7$ we obtained a pentagonal bipyramid [Fig. 3(a)] to be of lowest energy. The distance between its two apex atoms with coordination 6 is the shortest (5.3 a.u.) whereas the base atoms with coordination 4 have a bond length 6.04 a.u. Thus again the bonds connecting the ions with the largest coordination number are the shortest. This structure can be obtained from $Mg_6$ by capping the edge 3-4. Equivalently it can be obtained from $Mg_5$ by capping two adjacent faces such as 1-3-4 and 3-4-5.

A structure based upon another way of capping a tetrahedron is shown in Fig. 3(b). It is 0.019 eV/atom higher in energy than the pentagonal bipyramid. In this case

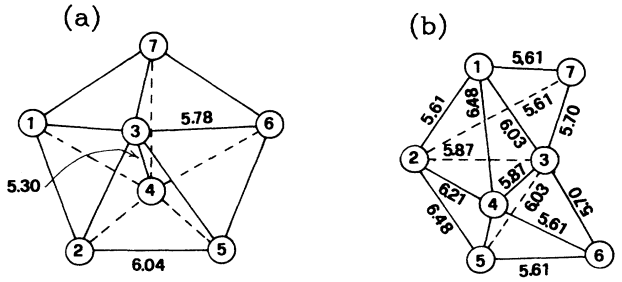


FIG. 3. Structures of $Mg_7$ cluster. (a) Pentagonal bipyramid and (b) another structure obtained from capping the trigonal bipyramid.

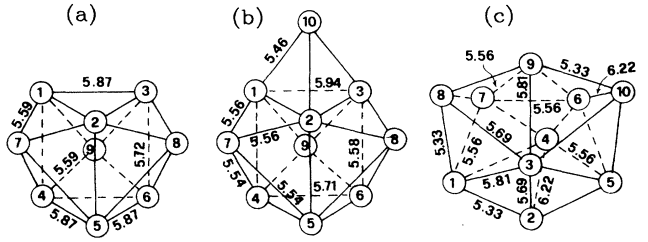


FIG. 5. Structures of (a) $Mg_9$ and (b) $Mg_{10}$ clusters. (c) Structure of $Mg_{10}$ obtained from the steepest-descent calculation starting with a geometry of $Be_{10}$ obtained in Ref. 22.

the bond lengths vary from 5.61 to 6.48 a.u. and there is no systematic trend as a function of the coordination. Thus our results agree with those of Reuse *et al.*[19] as well as with the configuration-interaction calculations of Pacchioni, Pewestorf, and Koutecky,[42] who also obtained a pentagonal bipyramid for this cluster.

### 4. $Mg_8$

The structure obtained from the simulated annealing is shown in Fig. 4(a). This can be simply obtained by capping a face (1-3-7 in the figure) of the pentagonal bipyramid. The bond lengths vary from 5.43 to 6.12 a.u. and there seems to be no systematic correlation with coordination number. This structure differs from the result of KW, who obtained a bicapped trigonal prism structure for $Be_8$. We have done a steepest-descent calculation starting with this structure for $Mg_8$ and the resultant relaxed geometry is shown in Fig. 4(b). This is 0.018 eV/atom higher in energy than the simulated annealing structure and has similarity with a fragment of the bulk Mg. One can see atoms 4-5-6-7-8 form part of a hexagon whereas 1 and 3 cap it as in the hcp or fcc structures. Therefore we find a different behavior for $Mg_8$ as compared to the one obtained for $Be_8$ by KW. This suggests that the progression of the bonding character is different in Mg as compared to Be clusters.

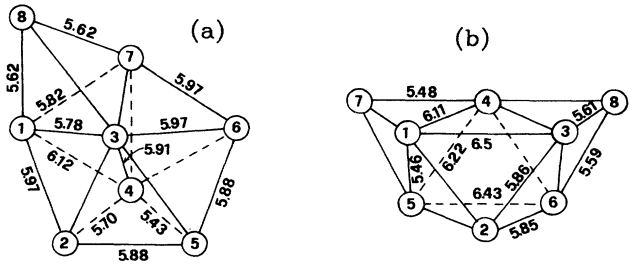


FIG. 4. Structures of $Mg_8$ cluster. (a) Capped pentagonal bipyramid and (b) the structure obtained from the steepest-descent calculation starting with a bicapped trigonal prism.

### 5. $Mg_9$ and $Mg_{10}$

$Mg_9$ is the first cluster where a new structure starts. It is a tricapped trigonal prism as shown in Fig. 5(a). No other structure was attempted for this cluster. It is, however, interesting to note that KW obtained the same structure for $Be_9$. This structure again has similarity with a strongly compressed fragment of the hcp lattice such that the bonds 1-4, 2-5, and 3-6 are much shorter than in the bulk Mg where they correspond to the $c$ axis.

Adding an atom to one of the triangular faces of the trigonal prism of $Mg_9$ leads to the structure of $Mg_{10}$ as shown in Fig. 5(b). This cluster has been studied independently by two other groups[43,44] who also obtained the same structure by the simulated annealing although their initial configurations were different. As we shall discuss later, this is the other most stable structure among the clusters we have studied and it is interestingly similar to the structure of $Si_{10}$ obtained by Ballone *et al.*[7] This coincidence may have an important implication from the point of view of the jellium model[45] and we shall discuss it in Sec. IV. However, for $Be_{10}$ KW's and our own calculations[46] predict a different structure than for $Mg_{10}$.

As a further check we carried out a steepest-descent calculation for $Mg_{10}$ starting with the $Be_{10}$ structure of KW. The resultant relaxed structure is shown in Fig. 5(c). It is only 0.005 eV/atom higher in energy than the simulated annealing structure and there are some structural similarities too. One can see a distorted trigonal prism of 1-3-5-7-9-6 atoms with 4, 8, and 10 capping its faces. The important difference is that in this structure the remaining atom caps an edge (3-4) whereas in Fig. 5(b) it caps a face (1-2-3). This structure can also be obtained from $Mg_8$ by further capping the two adjacent faces [compare Fig. 5(c) with Fig. 4(a)].

### 6. $Mg_{11}$

As $Mg_{10}$ is particularly stable, addition of an atom was found not to be favorable at the temperatures where MD runs were taken. This cluster showed a tendency for evaporation of an atom during the simulated annealing

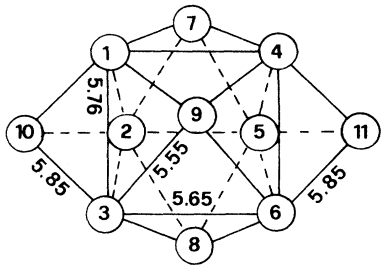


FIG. 6. Structure of $Mg_{11}$ obtained from the simulated annealing.

runs. A few independent runs led to the same behavior. Cooling and reheating of the cluster led to local minima where an atom was loosely attached to the cluster. The lowest-energy structure that we obtained is shown in Fig. 6. This structure can be obtained from $Mg_{10}$ by capping the remaining triangular face of the trigonal prism.

### 7. $Mg_{12}$

The structure obtained from the simulated annealing is shown in Fig. 7(a) and the bond lengths are presented in Table II, part (a). This structure can be obtained from an $Mg_9$ cluster by capping an edge (2-5) [atom 10 in Fig. 7(a)] and two faces (1-2-7 and 2-7-10). Capping the edge leads to an increase in the bond length of the edge. KW obtained a somewhat different structure for Be. Starting with their structure the steepest-descent calculations for $Mg_{12}$ lead to a structure which is shown in Fig. 7(b). This also differs from the structure of KW for $Be_{12}$. It is obtained from $Mg_9$ by capping the faces 1-4-7 and 2-5-7 and the edge 3-6 which gets elongated. The bond lengths are given in Table II, part (b). This structure is 0.036 eV/atom higher in energy than the one obtained from the simulated annealing. It again shows that Mg and Be have different growth behavior in this range of cluster size.

TABLE II. Bond lengths for the $Mg_{12}$ cluster obtained from (a) the simulated annealing and (b) the steepest-descent calculation using the geometry of Kawai and Weare (Ref. 22).

| (a) | | (b) | |
|---|---|---|---|
| Bonds | Distance (a.u.) | Bonds | Distance (a.u.) |
| 1-2 = 1-7 | 5.60 | 1-2 = 4-5 | 5.68 |
| 1-3 = 1-4 | 5.79 | 1-3 = 2-3 = 4-6 | 5.63 |
| 1-9 | 5.71 | 1-4 = 2-3 = 5-6 | 5.63 |
| 1-11 | 5.68 | 1-7 = 4-7 | 5.99 |
| 2-3 = 4-7 | 5.51 | 1-9 = 4-9 | 5.58 |
| 2-7 | 5.88 | 1-11 = 4-11 | 5.85 |
| 2-8 = 5-7 = 11-12 | 5.47 | 2-7 = 5-7 | 5.97 |
| 2-10 = 7-10 | 5.87 | 2-8 = 5-8 | 5.57 |
| 2-11 = 7-11 | 5.58 | 2-10 = 5-10 | 5.84 |
| 2-12 = 7-12 | 6.32 | 3-8 = 6-8 | 5.61 |
| 3-6 = 4-6 | 5.93 | 3-9 = 6-9 | 5.60 |
| 3-8 = 4-5 | 5.55 | 3-12 = 6-12 | 6.07 |
| 3-9 = 4-9 | 5.57 | 7-10 = 7-11 | 5.38 |
| 5-6 | 5.69 | 8-12 = 9-12 | 5.47 |
| 5-8 | 5.45 | | |
| 5-10 = 8-10 | 5.72 | | |
| 6-8 | 5.67 | | |
| 6-9 | 5.44 | | |
| 10-12 | 5.40 | | |

### 8. $Mg_{13}$

Several calculations were done for this cluster. It is generally considered that a 13-atom cluster is either an icosahedron or a cuboctahedron. However, simulated annealing calculations lead to a structure [Fig. 8(a)] which is neither of these. It can be considered to arise from the fusion of a $Mg_9$ (atoms 1 to 9) and a $Mg_4$ cluster (atoms 10 to 13). The tetrahedron of $Mg_4$ opens up to form a bent distorted rhombus. As discussed before, this is possible as there is no barrier for this distortion. The rhombus caps two adjacent faces (1-2-3 and 2-3-8 in the figure) of the capped trigonal prism. The bond lengths for this cluster are given in Table III, part (a). This structure can also be viewed as the fusion of a $Mg_{10}$ (atoms 1 to 10) and a $Mg_3$ (atoms 11 to 13) clusters. However, from the way $Mg_3$ fuses on $Mg_{10}$ we prefer to view it as the fusion of $Mg_9$ and $Mg_4$ clusters.

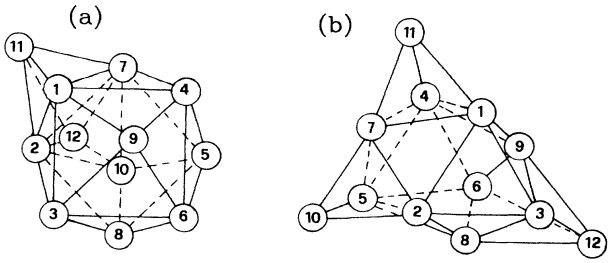


FIG. 7. Structures of $Mg_{12}$ obtained from (a) the simulated annealing and (b) the steepest-descent calculation starting with a geometry of $Be_{12}$ obtained in Ref. 22. For details see the text and Table II.

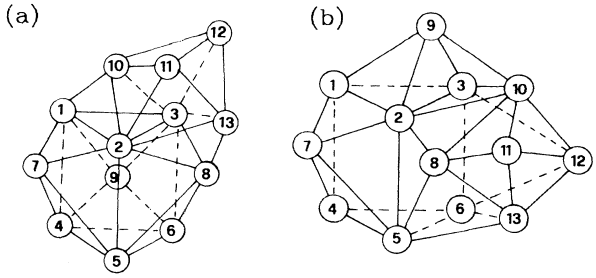


FIG. 8. Structures of $Mg_{13}$ obtained from (a) the simulated annealing and (b) the direct minimization of the hcp structure. For the bond lengths refer to Table III.

TABLE III. Bond lengths for the $Mg_{13}$ cluster obtained from (a) the simulated annealing and (b) the steepest-descent starting with a hcp structure.

| (a) | | (b) | |
|---|---|---|---|
| Bonds | Distance (a.u.) | Bonds | Distance (a.u.) |
| 1-2 | 5.71 | 1-2 | 6.38 |
| 1-3 | 5.73 | 1-3 | 6.33 |
| 1-4 | 5.74 | 1-4 | 5.53 |
| 1-7 = 1-9 | 5.58 | 1-7 = 1-9 | 5.47 |
| 1-10 = 11-13 | 5.48 | 2-3 | 6.60 |
| 2-3 | 5.84 | 2-5 | 5.43 |
| 2-5 = 2-10 = 3-10 | 5.86 | 2-7 = 12-13 | 5.66 |
| 2-7 = 3-9 | 5.51 | 2-8 = 2-10 = 9-10 | 5.56 |
| 2-8 = 8-13 | 5.60 | 3-6 | 5.31 |
| 2-11 | 7.07 | 3-9 | 5.44 |
| 2-13 | 6.09 | 3-10 | 5.51 |
| 3-6 | 5.85 | 3-12 | 5.88 |
| 3-8 | 5.62 | 4-5 | 5.70 |
| 3-12 | 6.77 | 4-6 | 5.78 |
| 3-13 | 6.08 | 4-7 | 5.55 |
| 4-5 = 4-6 | 5.55 | 5-6 = 11-12 | 5.50 |
| 4-7 = 4-9 = 10-11 | 5.59 | 5-7 | 6.03 |
| 5-6 | 5.87 | 5-8 | 5.57 |
| 5-7 = 6-9 | 5.44 | 5-13 | 5.98 |
| 5-8 = 6-8 | 5.49 | 6-12 = 6-13 = 8-13 | 5.73 |
| 10-12 | 5.62 | 8-10 = 8-11 = 10-11 | 5.68 |
| 11-12 = 12-13 | 5.50 | 10-12 | 5.85 |
| Bulk (Expt.) | 6.07 | 11-13 | 5.29 |

Steepest-descent calculations were also done with fcc, hcp, and icosahedron starting configurations. An interesting finding is that the hcp structure converges to a geometry [Fig. 8(b)] which has some similarity with the structure obtained from the simulated annealing and is only 0.005 eV/atom higher in energy. In this structure also one can see a trigonal prism of atoms 1 to 6 with some distortions but the capping is different [compare with Figs. 5(a) and 8(a)]. The faces 1-2-4-5 and 1-2-3 are capped by an atom each whereas the face 2-3-5-6 is covered by another with four atoms (8-10-12-13) rotated by about 90°. This is then capped by atom 11. The bond lengths for this structure are given in Table III, part (b). Considering this structure again as a fusion of a 9-atom cluster (atoms 1 to 9) and a 4-atom cluster [atoms 10 to 13 in Fig. 8(b)] we notice that the difference in the two structures in Fig. 8 is that in Fig. 8(a) atoms 8 and 9 cap a nearly square face of the trigonal prism whereas in the structure of Fig. 8(b) atom 9 caps a triangular face whereas 8 caps an edge. These results lead us to believe that out of the several ways in which a trigonal prism can be capped, in many cases the energies of the resulting structures may lie very close to each other as we find here. But the important point that emerges from these two calculations is that there may be a way of going from the simulated annealing structure to the hcp structure for larger clusters. For this to be confirmed calculations will be needed on larger clusters.

Relaxation of a fcc cluster leads to a significantly different structure as compared to the one obtained from the hcp and it lies 0.032 eV/atom higher in energy than the simulated annealing structure. Also relaxation of an icosahedron leads to a structure which is 0.043 eV/atom higher in energy than the one obtained from the simulated annealing. All the structures for 13-atom cluster have distortions and are not the closest packed such as an icosahedron expected for van der Waals bonded systems. This together with other results give a definite indication that the electronic structure plays the dominant role in the bonding of these clusters. However, the cohesive energy (Table I) is still about 54% of the bulk value (1.687 eV/atom) calculated by Moruzzi, Janak, and Williams[47] and larger clusters will be needed to get the bulklike behavior.

### B. Abundance of Mg clusters

To obtain the abundance of Mg clusters we calculated the quantity $\Delta = E(n+1) + E(n-1) - 2E(n)$ where E(n) is the total energy of the lowest-energy structure of a cluster with $n$ atoms. This is also shown in Fig. 9. It can be noted that the cohesive energy increases monotonically until $n = 10$. For $n = 11$ there is a small decrease in energy, then it starts slowly increasing. From the second derivative of the energy it is clear that 4- and 10-atom clusters are magic and should be abundant in the mass spectrum. These have 8 and 20 electrons, respectively, and correspond to the completion of shells in the spherical jellium model.[45] Clusters with 7 and 9 atoms should

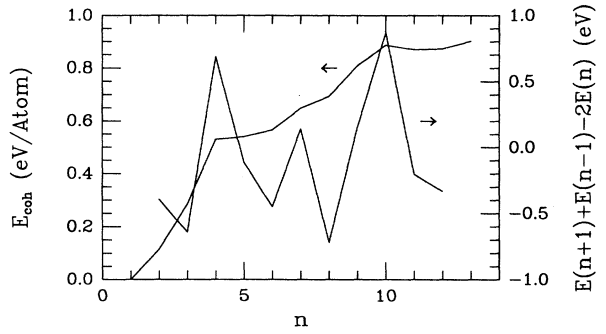


FIG. 9. Plot of the cohesive energy (left scale) and its second derivative (right scale) as a function of the cluster size.

also be abundant though less so as compared to 4 and 10. These correspond to 14 and 18 electrons and are also expected to be abundant in the ellipsoidal shell model.[48] [In fact, 18 electrons correspond to the completion of the $1d$ shell in the spherical jellium model but the relative stability of the 18- and 20-electron systems will depend on the distribution of the eigenstates (see Fig. 12).] It may be worth noting that for Na clusters[49] in addition to the strong peaks at $n = 8$ and 20, prominent peaks were also observed for $n = 14$ and 18 clusters. Thus our results support the general predictions of the shell model. The spherical jellium model calculations of Chou and Cohen[50] for Mg predict $Mg_{10}$ to be the smallest abundant cluster. However, 4- and 7-atom clusters may be too small to be treated well in a spherical jellium model. Though our lowest-energy structures for the 4- and 7-atom clusters are the same (except for some bond lengths) as for the van der Waals bonded systems, our calculations of the electronic charge densities suggest that the bonding in these clusters is more covalent-metallic-like. A further discussion on the nature of bonding that we find from our calculations will be given in Sec. III D.

The 11-atom cluster has the tendency of disintegration into a 10-atom cluster and an atom and therefore under the experimental conditions may not be present in the mass spectrum. Figure 10 shows the energy for fragmentation of the Mg clusters. Results are presented only for monomer and dimer dissociation. It is clear that the most favorable channel is the monomer dissociation.

### C. Chemisorption energy

An understanding of the variation in the chemisorption properties of clusters is important for catalysis. Also several calculations of chemisorption behavior are done using a cluster as representative of the bulk. We consider Mg chemisorption on Mg clusters as a model to study its size dependence. Since we take directly the results of our optimized geometries, any relaxation and/or structural transformation that may occur on chemisorption is automatically included. In Fig.11 we show the behavior of the chemisorption energy defined as $E_{\rm chem}(n) = |E(n+1) - E(n) - E(1)|$ as a function of the cluster size. While a strong variation is evident, an important point is that if the addition of an atom to a nonmagic (for example, 3, 6, and 8 here) cluster makes it a magic one then the chemisorption energy is large. Also for $Mg_9$ the chemisorption energy is large as $Mg_{10}$ is magic, whereas for magic clusters the chemisorption energy is particularly small. This can be noted in particular for 4- and 10-atom clusters. It also agrees with a recent study[51] of oxygen chemisorption on Al clusters. It has been noted that magic anion clusters of aluminium such as $Al_{13}^-$ remain inert under oxygen exposure whereas the intensity of other clusters decreases very significantly, obviously due to a reaction with oxygen. $Al_{13}^-$ has 40 electrons and corresponds to a shell closing in the jellium model. Therefore according to our results it should be less reactive. This behavior of clusters can play a very important role in tailoring catalysts for a particular reaction.

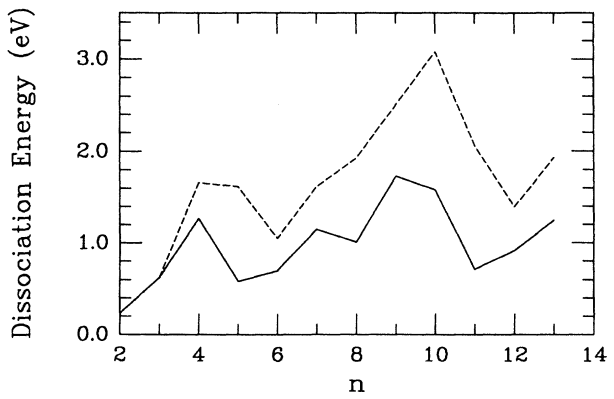


FIG. 10. Dissociation energy $E_{n-m} + E_m - E_n$ as a function of the cluster size. Solid lines denote monomer ($m = 1$) fragmentation and dashed lines denote dimer ($m = 2$) fragmentation.

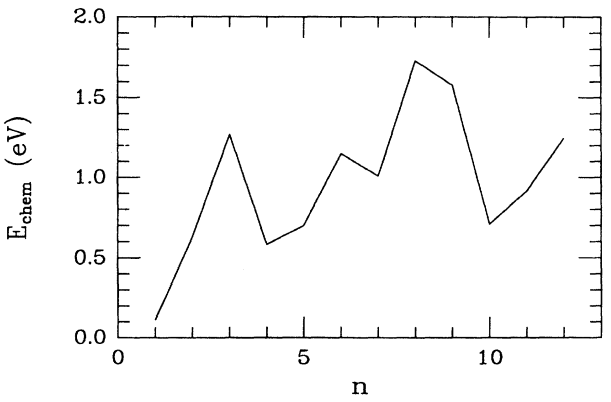


FIG. 11. Chemisorption energy of Mg on $Mg_n$ clusters as a function of the cluster size.

### D. Bonding characteristics

An important question for clusters of divalent metals is the understanding of the transition from van der Waals or weak chemical bonding to metallic behavior. We have tried to understand the nature of bonding in these clusters from the gap between the highest occupied and the lowest unoccupied Kohn-Sham eigenstates, the build-up of the $p$ character of the electronic charge, the distribution of electron charge densities and the behavior of the nearest-neighbor bond lengths. All these results lead to the following coherent picture of the nature of bonding.

For metallic behavior we expect that (1) there should be a significant overlap of the electron charge densities of the atoms and consequently an increase in the $p$ character and (2) the gap between the highest occupied and the lowest unoccupied states should become small. In Fig. 12 we present the Kohn-Sham eigenvalues for different clusters and in Fig. 13 the gap between the highest occupied and the lowest unoccupied states. For the magic clusters which also have high symmetry, the states are bunched together whereas for nonmagic clusters they are spread. The gap shows an oscillatory behavior and is largest for the dimer as one can expect for a van der Waals or weakly bonded cluster. It then gradually decreases but for clusters corresponding to shell closing in the jellium model, the gap shows a local maximum with an exception of $n = 9$. For $n > 10$ the gap is rather small. As we mentioned in Sec. II, these were the clusters which showed a tendency for metallization in the MD runs. However, even for larger clusters the gap is expected to show an oscillatory behavior and may remain significant for bigger magic clusters since the convergence to the bulk cohesive energy is rather slow.

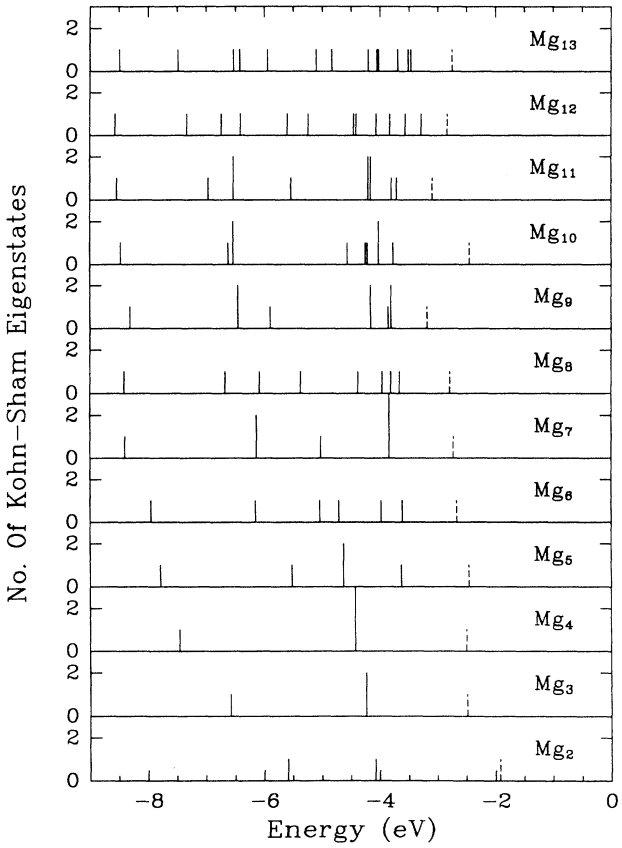


FIG. 12. Plots of the Kohn-Sham eigenvalues for $Mg_n$ clusters correspond to the lowest-energy structures of $n = 2$ to 13 clusters. The dashed line shows the lowest unoccupied state.

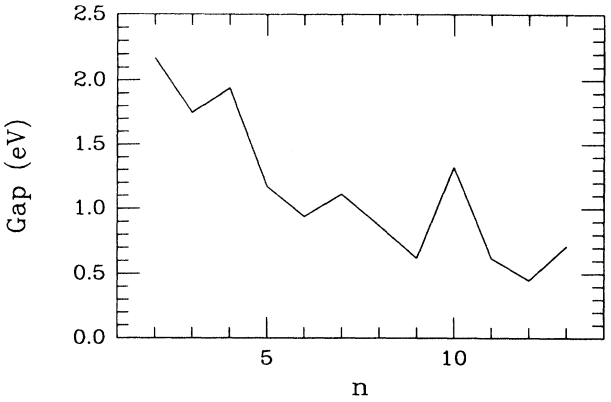


FIG. 13. Gap between the highest occupied and the lowest unoccupied eigenstates as a function of the cluster size as obtained from Fig. 12.

The variation of the nearest-neighbor bond lengths, the number of bonds per atom and the $p$ character of the pseudoelectronic charge density is shown in Fig. 14. For the dimer the bond length is even larger than the nearest-neighbor distance in the bulk (5.95 a.u. as obtained by Moruzzi, Janak, and Williams[47]) and the bonding is very weak. The bond length decreases until $n = 4$ [Fig. 14(a)] and then increases and again a minimum is obtained for $n = 10$. Thereafter the bond length varies slightly but is smaller than expected for the bulk. This behavior of the bond length obtained here seems to us to be a property of a system showing a transition from van der Waals or weak chemical bonding to metallic behavior. A simple reason for this behavior is that for weakly bonded clusters the bond distances are much larger as compared to the bulk of the same material (having metallic behavior) whereas for clusters[52] and surfaces[53] of metallic systems bond distances are shorter than in the bulk. Thus until metallization occurs in the cluster, there will be a tendency for decreasing the mean bond length until a critical cluster size is reached where the cluster starts behaving like a metal. For clusters larger than this critical size the mean bond length should tend to increase towards its bulk value. The oscillatory behavior and the local minimum in the mean bond length for $n = 4$ and 10 seems to us to be related to the shell closing. The number of bonds per atom show a rather smooth behaviour and it increases almost monotonically as the size of the cluster increases.

The $p$ character of the electronic pseudocharge for the

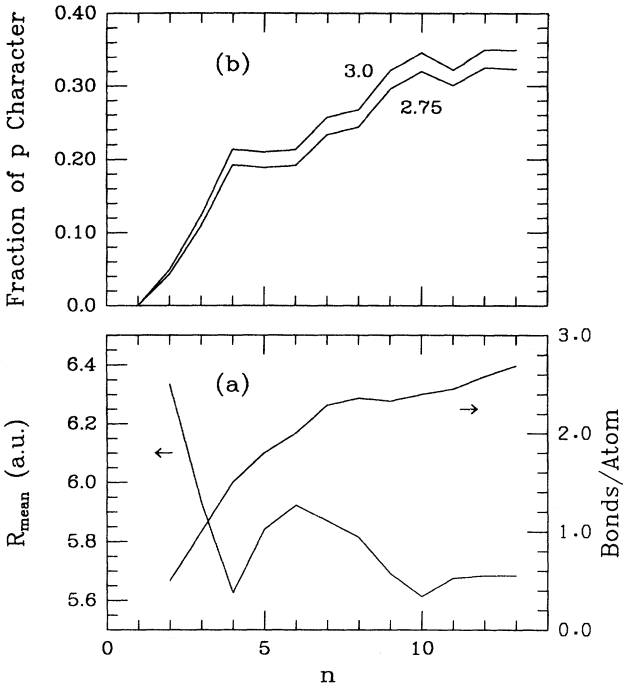


FIG. 14. Plot of (a) the mean nearest-neighbor bond lengths (left scale) and the number of nearest-neighbor bonds per atom (right scale) as a function of the cluster size for the lowest-energy structures and (b) the fraction of the $p$ to the $s$ and $p$ characters of the electronic pseudocharge densities of the clusters for two values of the radius of spheres around ions over which the integration was performed to calculate the total pseudocharge.

clusters is shown in Fig. 14(b). This has been obtained by projecting the pseudo-wave-functions on spherical harmonics centered at different ions. The $s$ and $p$ electronic pseudocharges were then calculated by integrating the projected pseudocharge densities within a sphere of radius $R$ around each atom. The fraction of the $p$ character is shown in Fig. 14(b) for $R$=2.75 and 3.0 a.u. These two values of $R$ represent half the mean bond lengths present in all the clusters with $n > 2$. The overall trends in both the cases are the same[54] and show a good correlation with the mean bond length in the cluster. If the mean bond length in a cluster decreases (increases) then there is an increase (decrease) in the $p$ character. It can be noted that there is a sudden buildup of the $p$ character as the cluster size increases from 2 to 4 atoms which also corresponds to a decrease in the bond lengths. Then for the 5-atom cluster there is a small decrease in the $p$ character which also corresponds to an increase in the mean bond length. As the mean bond length decreases in going from a 6- to a 10-atom cluster the $p$ character increases and again for an 11-atom cluster it decreases since the mean bond length increases slightly. In order to understand it better two factors can be considered to contribute to the development of the $p$ character: (1) the mean coordination which increases [Fig. 14(a)] with the cluster size and leads to an increase in the $s - p$

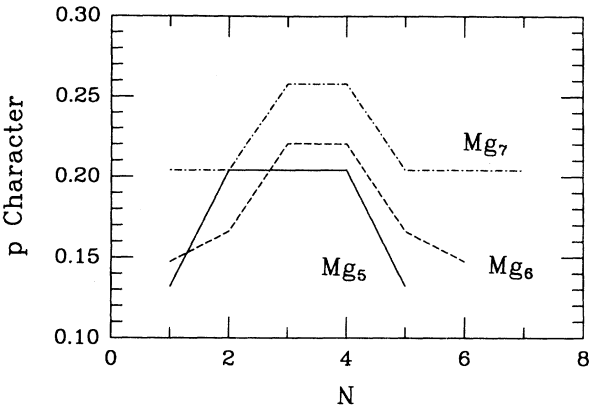


FIG. 15. $p$ character of the electronic pseudocharge densities around ions ($N$) in $Mg_n$ clusters. $n = 5$ (solid line); $n = 6$ (dashed line); $n = 7$ (dash-dotted line). Here $N$ refers to the number of an ion as shown in Figs. 1–3 for the lowest-energy structures.

hybridization and (2) the variation of the bond lengths whose effect is more significant as can be seen for the 5-atom cluster. In this case the number of nearest-neighbor bonds per atom increases to 1.8 as compared to 1.5 for $Mg_4$, but there is a small decrease in the $p$ character of the cluster due to an increase in the mean bond length. The $p$ character of the charge density surrounding each ion, however, shows (Fig. 15) that the three base atoms (with short bond lengths) have more $p$ character than the apex atoms. Similarly for the 6- and 7-atom clusters the atoms connected with the shortest bonds have the highest $p$ character and therefore *the bonding character has local variations in clusters.* We suggest that as the cluster growth progresses, metallization occurs in such short bonds first.

To further illustrate the bonding nature for smaller clusters we show in Figs. 16(a), 17(a), and 18(a) the electronic pseudocharge density contours for the base in 3-, 4-, and 7-atom clusters. It can be seen that for 3- and

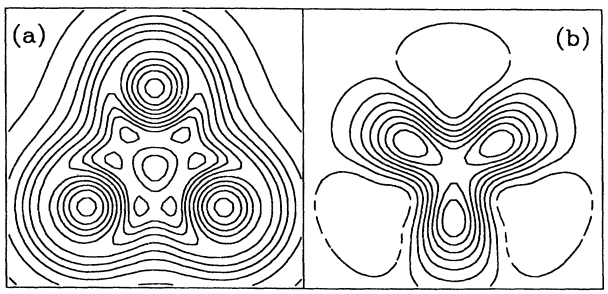


FIG. 16. (a) Pseudocharge density contours for the $Mg_3$ equilateral triangle in the plane of the cluster. (b) The difference in the self-consistent and the overlapping atomic pseudocharge densities. Solid (dashed) contours represent excess (depletion) of the charge.

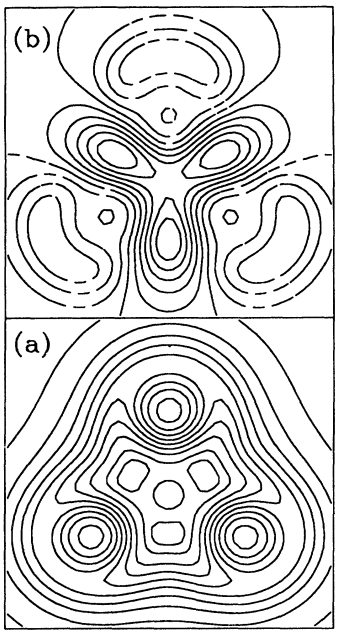


FIG. 17. Same as in Fig. 16 for $Mg_4$ in the plane of the base atoms.

4-atom clusters there is a build up of the pseudocharge along the bonds as in covalent systems. This moves toward the center of the cluster and gets more delocalized as the cluster size grows. Figures 16(b), 17(b), and 18(b) show the difference in the calculated and the overlap of the atomic pseudocharge densities which again confirm these conclusions. This behavior suggests a gradual development of covalent to metallic bonding in these clusters and before a transition to complete metallic bonding occurs, different atoms in the cluster have different bonding characteristics.

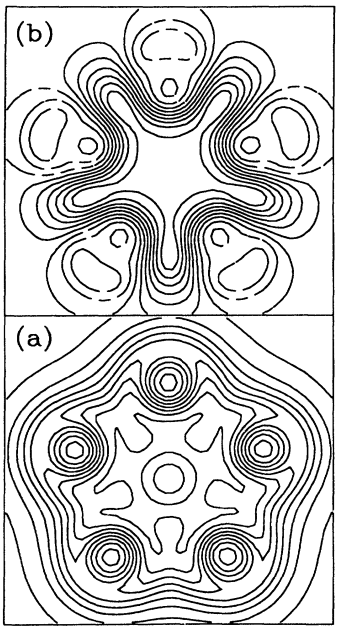


FIG. 18. Same as in Fig. 16 for $Mg_7$ in the plane of the base atoms.

## IV. DISCUSSION AND CONCLUSIONS

The structures of Mg clusters can be described in terms of a tetrahedron and a trigonal prism. Up to 8-atom clusters growth is by capping the faces of a tetrahedron whereas for bigger clusters the capping of a trigonal prism becomes more favorable. It is interesting to note that for Be clusters a recent calculation[22] also finds a tetrahedron and a trigonal prism to be the two basic structures. But the growth behavior is different for $n > 7$. For Be clusters edge capping is favored over face capping for some clusters.

Some Mg clusters are found to resemble a fragment of the hcp structure. However, the transition to bulk behavior is slow. Another important result is that a 13-atom cluster with a starting hcp structure leads to a geometry which is nearly degenerate to the one obtained from the simulated annealing and also has some structural similarities. Structures obtained from relaxing the fcc and the icosahedron clusters have significantly higher energies. This suggests the possibility of a path for transition to the hcp structure for larger clusters.

For Mg 4-, 7-, 9-, and 10-atom clusters are magic, which is in general agreement with the jellium model of the metal clusters. The result that $Mg_{10}$ and $Si_{10}$ have the same structure may have important consequences for the magic clusters. Bulk Mg is metallic whereas Si is covalently bonded. However, there may be some interesting similarities when they are in the form of small clusters. $Mg_{10}$ has 20 valence electrons while $Si_{10}$ has 40. From the point of view of the jellium model[45] both these electron numbers correspond to a shell closing and the corresponding clusters are expected to be magic. It is also important to note that $Si_9$ which has 36 valence electrons and is nonmagic, has a different structure[7] as compared to $Mg_9$. These results raise an interesting possibility of occurence of some unique structures for metal or metal-like clusters when an electronic shell is complete. However, one has to be careful about the validity of the jellium model since both Mg and Si clusters involve a change in the bonding character as the cluster size grows. It should be mentioned that $Si_5$ with 20 valence electrons is not a magic cluster. Also $Be_{10}$, which has 20 electrons, has a different structure than $Mg_{10}$. This may, however, be due to the fact that Be clusters tend to achieve bulklike structure in this range.

Regarding the nature of the bonding in these clusters, we find that different atoms in a cluster have different bonding characters. There are a few short bonds in the clusters where the metallization occurs first. These are the atoms whose coordination is highest so that the mixing of the $s$ and the $p$ states is large. The increase in the $p$ character of the charge in Mg clusters is slower as compared to Be and therefore in the case of Mg larger clusters will be needed to obtain bulklike behavior.

In the range of the clusters we have studied, the approach to bulk bonding character is oscillatory. The mean nearest-neighbor bond length also shows an oscillatory trend as the cluster size grows. We conjecture this to be a typical behavior for clusters showing a transition from van der Waals or weak chemical to metallic bonding. The gap between the highest occupied and the lowest unoccupied states shows a large variation which should show up in the optical properties of these clusters. The gap is large for magic clusters and decreases as the magic cluster size increases. However, for some intermediate nonmagic clusters the gap can become quite small and can lead to an interesting variation in the physical properties. The chemisorption energy also shows an oscillatory behaviour and in particular the magic clusters are found to be less reactive. Regarding fragmentation, for Mg clusters monomer dissociation is most favorable. In particular $Mg_{n+1}$ clusters with $n$ corresponding to a magic cluster are found to be more likely to show fragmentation.

In conclusion we have studied the structure and the growth behavior of Mg clusters with up to 13 atoms and find interesting variations in the bonding properties. The growth behavior of Mg clusters is different from Be. Striking similarities are seen in the structures obtained from the simulated annealing and the direct steepest-descent minimization of the hcp structure of a 13-atom cluster. This suggests the possibility of a path for transition to bulklike structure for bigger clusters. However, further calculations on bigger clusters will be needed to find when such a transition will occur. The convergence to bulk behavior is oscillatory and slow. However, we shall like to emphasize that the question when a transition to metallic behavior occurs will depend on the physical property one is interested in. Our calculations also point out the possibility of some unique structures for magic clusters of metal or near metallic systems and it would be of interest to explore it.

## ACKNOWLEDGMENTS

One of us (V.K.) would like to thank the members of the Condensed Matter Sector, SISSA and the Computer Centre, ICTP for their help and cooperation at various stages of this work. Specially he would like to thank Guilia Galli for her help in the initial stages of this project and to M. Parrinello, G. Chiarotti, and G. Pastore for helpful advice. This work was started when V.K. was visiting the ICTP, Trieste, and has been completed in subsequent short visits. He would like to thank Professor Abdus Salam, the International Atomic Energy Agency, the UNESCO, and the SISSA for their hospitality in Trieste. This work has been supported in part by the Scuola Internazionale Superiore di Studi Avanzati-Centro di Calcolo Elettronico dell'Italia Nord-Orientale collaborative project, under the sponsorship of the Italian Ministry for Public Education.

*On leave from Materials Science Division, Indira Gandhi Centre for Atomic Research, Kalpakkam 603 102, India.

†Present address: IRRMA, CH-1015 Lausanne and Department of Condensed Matter Physics, University of Geneva, CH-1211 Geneva, Switzerland.

[1] *Microclusters*, edited by S. Sugano, Y. Nishina, and S. Ohnisi (Springer, Berlin, 1987).

[2] *Physics and Chemistry of Small Clusters*, Vol. B158 of *NATO Advanced Study Institute, Series B: Physics*, edited by P. Jena, B. K. Rao, and S. N. Khanna (Plenum, New York, 1987).

[3] *Elemental and Molecular Clusters*, edited by G. Benedek, T. P. Martin, and G. Pacchioni (Springer, New York, 1988).

[4] Articles in the Proceedings of the Fourth International Meeting on Small Particles and Inorganic Clusters, Marseille, France, 1988 [Z. Phys. D **12** (1989)].

[5] Proceedings of the International Conference on Inorganic Clusters and Small Particles, Konstanz, 1990 [Z. Phys. D **19** (1991); D **20** (1991)].

[6] W. Kratschmer, D. L. Lowell, K. Fostiropoulos, and D. R. Huffman, Nature **347**, 354 (1990).

[7] P. Ballone, W. Andreoni, R. Car, and M. Parrinello, Phys. Rev. Lett. **60**, 271 (1988).

[8] D. Tomanek and M. A. Schluter, Phys. Rev. B **36**, 1208 (1987).

[9] J. R. Chelikowsky, Phys. Rev. Lett. **60**, 2669 (1988).

[10] W. Andreoni (private communication).

[11] K. Rademann, B. Kaiser, U. Even, and F. Hensel, Phys. Rev. Lett. **59**, 2319 (1987); K. Rademann, Ber. Bunsenges. Phys. Chem. **93**, 653 (1989); C. Brechignac, M. Broyer, P. Cahuzac, G. Delacretaz, P. Labastie, J. P. Wolf, and L. Woste, Phys. Rev. Lett. **60**, 275 (1988).

[12] J. C. Phillips, Chem. Rev. **86**, 619 (1986).

[13] See, e.g., K. D. Jordan and J. Simons, J. Chem. Phys. **65**, 1601 (1976); J. C. Miller, B. S. Ault, and L. Andrews, *ibid.* **67**, 2478 (1977).

[14] F. Maeder and W. Kutzelnigg, Chem. Phys. Lett. **37**, 285 (1976).

[15] R. O. Jones, J. Chem. Phys. **71**, 1300 (1979); R. O. Jones and O. Gunarsson, Rev. Mod. Phys. **61**, 689 (1989).

[16] K. A. Gschneidner, Jr., Solid State Phys. **16**, 276 (1964).

[17] K. P. Huber and G. Herzberg, *Molecular Spectra and Molecular Structure. IV. Constants of Diatomic Molecules* (Van Nostrand Reinhold, New York, 1974).

[18] For $Be_2$ see V. E. Bondybey and J. H. English, Chem. Phys. Lett. **94**, 443 (1983).

[19] F. Reuse, S. N. Khanna, U. de Coulon, and J. Buttet, Phys. Rev. B **41**, 11 743 (1990).

[20] S. N. Khanna, F. Reuse, and J. Buttet, Phys. Rev. Lett. **61**, 535 (1988).

[21] See also C. W. Bauschlicher, Jr., P. S. Bagus, and B. N. Cox, J. Chem. Phys. **77**, 4032 (1982); G. Pacchionni and J. Koutecky, *ibid.* **77**, 5850 (1982); P. S. Bagus, C. J. Nelin, and C. W. Bauschlicher, Surf. Sci. **156**, 615 (1985).

[22] R. Kawai and J. H. Weare, Phys. Rev. Lett. **65**, 80 (1990).

[23] V. Kumar, in *Proceedings of the Anniversary Adriatico Research Conference on Quasicrystals*, edited by M. Jaric and S. Lundquist (World Scientific, Singapore, 1990), pp. 391.

[24] See articles in Proceedings of the International Workshop on Quasicrystals, Beijing, 1987 [Mater. Sci. Forum **22-24**

(1987)].
[25] R. Car and M. Parrinello, Phys. Rev. Lett. **55**, 2471 (1985).
[26] W. Andreoni and G. Pastore, Phys. Rev. B **41**, 10 243 (1990).
[27] D. Hohl, R. O. Jones, R. Car, and M. Parrinello, Chem. Phys. Lett. **139**, 540 (1987).
[28] D. Hohl, R. O. Jones, R. Car, and M. Parrinello, J. Chem. Phys. **89**, 6823 (1988).
[29] P. Ballone, W. Andreoni, R. Car, and M. Parrinello, Europhys. Lett. **8**, 73 (1989).
[30] R. O. Jones and D. Hohl, J. Chem. Phys. (to be published).
[31] W. Andreoni (private communication).
[32] V. Kumar, R. Car, and M. Parrinello, in Proc. Solid State Phys. Symp. (India) **32C**, 133 (1989).
[33] V. Kumar and R. Car, in Proceedings of the International Conference on Inorganic Clusters and Small Particles (Ref. 5); Z. Phys. D **19**, 177 (1991).
[34] R. Car and M. Parrinello, in *Simple Molecular Systems at Very High Density*, Vol. B186 of *NATO Advanced Study Institute, Series B: Physics*, edited by A. Polian, P. Loubeyre, and N. Boccara (Plenum, New York, 1989).
[35] J. P. Perdew and A. Zunger, Phys. Rev. B **23**, 5048 (1981).
[36] D. M. Ceperley and B. J. Alder, Phys. Rev. Lett. **45**, 566 (1980).
[37] G. B. Bachelet, D. R. Hamann, and M. Schluter, Phys. Rev. B **26**, 4199 (1982).
[38] L. Kleinman and D. M. Bylander, Phys. Rev. Lett. **48**, 1425 (1982).
[39] The change in the energy and the bond length in going from 6 to 8 Ry was about 0.15%.
[40] For 7- and 11-atom clusters we noted a tendency for the evaporation of an atom. In such cases more care is required during the simulated annealing runs as one can get trapped in some metastable states.
[41] M. R. Hoare and P. Pal, Adv. Phys. **20**, 161 (1971); J. Farges, M. F. de Feraudy, B. Raoult, and G. Torchet, J. Chem. Phys. **78**, 5067 (1983); **84**, 3491 (1986).
[42] G. Pacchioni, W. Pewestorf, and J. Koutecky, Chem. Phys. **83**, 261 (1984).
[43] W. Andreoni (private communication).
[44] P. Ballone *et al.*, in Proceedings of the International Conference on Inorganic Clusters and Small Particles (Ref. 5); Z. Phys. D **19**, 173 (1991).
[45] W. A. de Heer, W. D. Knight, M. Y. Chou, and M. L. Cohen, *Solid State Physics*, edited by H. Ehrenreich and D. Turnbull (Academic, New York, 1987), Vol. 40.
[46] V. Kumar and R. Car (unpublished).
[47] V. L. Moruzzi, J. F. Janak, and A. R. Williams, *Calculated Electronic Properties of Metals* (Pergamon, New York, 1978).
[48] K. Clemenger, Phys. Rev. B **32**, 1359 (1985).
[49] W. D. Knight, K. Clemenger, W. A. de Heer, W. A. Saunders, M. Y. Chou, and M. L. Cohen, Phys. Rev. Lett. **52**, 2141 (1984).
[50] M. Y. Chou and M. L. Cohen, Phys. Lett. **113A**, 420 (1986).
[51] R. E. Leuchtner, A. C. Harms, and A. W. Castleman, Jr., J. Chem. Phys. **91**, 2753 (1989).
[52] See, e.g., G. Apai, J. F. Hamilton, J. Stohr, and A. Thompson, Phys. Rev. Lett. **43**, 165 (1979); J. R. Noonan and H. L. Davis, Phys. Rev. B **29**, 4349 (1984), and references therein; J. W. M. Frenken, J. F. van der Veen, and G. Allen, Phys. Rev. Lett. **51**, 1876 (1983).
[53] See, e.g., B. Delley, D. E. Ellis, A. J. Freeman, E. J. Baerends, and D. Post, Phys. Rev. B **27**, 2132 (1983); K. M. Ho and K. P. Bohnen, *ibid.* **32**, 3446 (1985).
[54] A fraction of the charge still remains outside the sphere of integration. However, we expect that the general trends shown here will not be affected much if this is included.